# On the Theory of Grafted Weak Polyacids

**R. Israëls,* F. A. M. Leermakers, and G. J. Fleer**

*Department of Physical and Colloid Chemistry, Wageningen Agricultural University, Dreijenplein 6, 6703 HB Wageningen, The Netherlands*

*Received December 4, 1993; Revised Manuscript Received March 11, 1994*[⊕]

ABSTRACT: We use a self-consistent mean-field (SCF) theory to determine the behavior of grafted polyacids. In these systems, the charge on a brush segment depends on its local environment and on the pH of the solution. The scaling dependence of the brush height on salt concentration $\phi_s$ is significantly different from that for a brush with constant charge density. In the latter case, the thickness is a continuously decreasing function of $\phi_s$, whereas for a brush of weak polyacids the thickness passes through a maximum. The numerical SCF results show qualitative agreement with predictions obtained from a simple scaling model based upon a block profile with a uniform degree of dissociation.

## I. Introduction

Over the past few years, the properties of brushes have received a great deal of attention (see ref 1 for a review). It is now well established that the thickness of a brush is proportional to the chain length[2] and that the segments in an uncharged brush experience a potential which is a parabolic function of the distance from the surface. In a good solvent, where this potential is proportional to the volume fraction of brush segments, this leads to a parabolic segment density profile,[3,4] whereas in poorer solvents a more condensed volume fraction profile is predicted.[5]

Much less work has been done on brushes where the polymers carry charges.[6-8] In a recent contribution[9] the structure of a brush in which the segments carry a constant charge was investigated in detail, both in the absence and in the presence of salt. When the brush is in equilibrium with a salt-free solution, it can be described as an *osmotic brush* (OsB). At higher concentrations of external salt a *salted brush* (SB) may be found, which can be described as a neutral brush with a (high) *effective* excluded-volume parameter. In an excess of electrolyte, the charges are largely screened and the *quasi neutral brush* (QNB) regime can be found.

In this paper we extend this treatment to brushes carrying *weak* groups (e.g., carboxylic groups), for which the degree of dissociation is a function of the local pH. One important consequence is that, at low ionic strength, the segments in such a brush are much more weakly charged than those in a brush with fixed charges. Under salt-free conditions most of the segments associate with a proton in order to minimize the free energy of the brush in the high electrostatic potential generated by the few remaining charges. Hence, paradoxically, a brush of a weak polyacid becomes a neutral brush in the absence of salt.

We are not aware of any theory that predicts how the properties of these brushes depend on the important system parameters. In many practical applications, local regulation of charges in brushes is important. For example, in biological systems, where (charged) brushlike structures are frequently found, the local salinity and pH are carefully maintained and the extension of the brush might be under active control.

Another example where the subject of this paper is of relevance is the stability of core–shell latices. Polyelectrolyte shells are often used to make hydrophobic latices water-compatible. The extension of the shell layer can then be controlled by ionic strength and, when the charges are weak, by the pH of the solution. Detailed predictions of how these parameters determine the brush properties are of considerable importance and will help to tune these brushes for specific applications.

We analyze brushes using a numerical self-consistent-field (SCF) model. It is derived from the Scheutjens–Fleer model,[17,18] which describes the adsorption of uncharged homopolymers. We include electrostatic interaction using the multilayer Stern model[10,12] and employ the so-called two-state approach to describe the acid–base equilibrium of weakly charged segments. The latter approach was originally developed by Björling et al.[13] to describe the anomalous phase behavior of poly(ethylene oxide) molecules in terms of an equilibrium between two states that are assumed to have a different solvency. We apply the two-state model to segments that may be either charged or uncharged in order to model the acid–base equilibrium of these segments. The two-state model as derived by Björling can be simplified considerably, as has been shown by Hurter.[15] In Appendix A we show this approach to be valid if monomers are considered. The validity for the monomeric case is also a rigorous proof for the polymeric case, since in our SCF model the energetic interactions can be separated from the chain statistics.

We introduce the SCF model in section II. In section III we derive the scaling relations for the layer height using the (approximate) assumptions of a block profile and uniform dissociation for all segments. Subsequently, in section IV we compare the results of the two approaches, and in section V we provide a summary of the main conclusions.

## II. Numerical Model

In the SCF model we divide the half-space next to a surface into parallel layers of thickness $d$, numbered $z = 1, 2, ..., M$ where $M$ is sufficiently large. A central parameter is the weighting factor $G_A(z)$ for a segment A in layer $z$, defined as the statistical weight of finding a free segment of type A in layer $z$. If such a segment can be in only one state, the weighting factor is given by

$$G_A(z) = e^{-u_A(z)/kT} \tag{1}$$

where $u_A(z)$ is the potential of mean force, with respect to a reference state that we take to be the bulk solution. (Obviously, for the present brush system, the concentration of A segments in the bulk equals zero. Still, the weighting

[⊕] Abstract published in *Advance ACS Abstracts,* April 15, 1994.

0024-9297/94/2227-3087$04.50/0 © 1994 American Chemical Society

factor can be defined with respect to the bulk as $G_A(z) = \exp[(u_A(z) - u_A^b)/kT]$, where $u_A^b$ is the reference potential for A segments. Similarly, $\alpha^b$ gives the (virtual) degree of dissociation in this reference state.) The end-point distributions of the chains can be calculated from $G_A(z)$ along the lines of the Scheutjens–Fleer theory.[10,17,18] In this method all allowed conformations of chain molecules are generated in a first-order Markov approximation; direct chain backfolding is permitted. Grafted polymers are modeled by allowing only those chain conformations that have their first segment in layer $z = 1$ and by fixing the total number of polymer units in the system.[19] Three additional components, water, positively charged ions, and negatively charged ions, are allowed in each lattice layer. These monomeric components are free to leave the brush region. Consequently, for these components the concentration in the bulk solution is the input parameter.

The electrostatic potential can be expressed in terms of the local concentrations using the multilayer Stern model. For details and the numerical procedure for solving the equations self-consistently, we refer to the literature.[10–12,20]

In the present paper, instead of having a constant charge on the brush segments, we consider the following acid–base equilibrium:

$$HA \rightleftharpoons A^- + H^+ \tag{2}$$

In this equilibrium, HA is an uncharged acidic brush segment, $A^-$ a negatively charged segment, and $H^+$ a proton. This equilibrium is characterized by a constant $K_a$, defined as:

$$K_a = \frac{[H^+][A^-]}{[HA]} \tag{3}$$

where the square brackets denote a concentration. The degree of dissociation $\alpha$ is generally defined as:

$$\alpha = \frac{[A^-]}{[A^-] + [HA]} \tag{4}$$

In the SCF model, we have to consider this acid–base equilibrium in each of the layers $z = 1, ..., M$, as well as in the reference state, and find an expression for the *effective* weighting factor $G_A(z)$ for A segments that can be in two states. According to the two-state model, it is given by[13,15] (see also Appendix A):

$$G_A(z) = \alpha^b G_{A^-}(z) + (1 - \alpha^b) G_{HA}(z) \tag{5}$$

$G_{HA}(z)$ and $G_{A^-}(z)$ are the true weighting factors for HA and $A^-$ segments, respectively. The degree of dissociation in the reference state, $\alpha^b$, is an input parameter for the theory. We may express it in terms of $K_a$ and $[H^+]$, where $[H^+]$ (without the argument $z$) will henceforth denote the *bulk* concentration of protons:

$$\alpha^b = \frac{K_a}{K_a + [H^+]} \tag{6}$$

Note that it is only the ratio $K_a/[H^+]$ which is important.

The dissociation in layer $z$ is defined by eq 4, provided $[A^-]$ and $[HA]$ are the *local* concentrations. It may be written as[16] (see also Appendix A):

$$\alpha(z) = \alpha^b G_{A^-}(z)/G_A(z) \tag{7}$$

In our calculations we take nonelectrostatic contributions (solvency and adsorption energy) to be identical for HA and $A^-$. Then the ratio $G_{A^-}(z)/G_{HA}(z)$ is simply expressed as a Boltzmann factor of the local electrostatic potential $y(z)$:

$$G_{A^-}(z)/G_{HA}(z) = e^{y(z)} \tag{8}$$

where $y(z)$ is expressed in units $kT$ per elementary charge $e$ to make it dimensionless. For a polyacid brush, this electrostatic potential $y(z)$ is negative with respect to the bulk solution, and $G_{A^-}(z)$ is smaller than $G_{HA}(z)$. Now we can rewrite eq 7 by substitution of eqs 5, 6, and 8 as

$$\alpha(z) = \frac{K_a}{K_a + [H^+]e^{-y(z)}} \tag{9}$$

which is fully consistent with the local version of eq 6, obtained by replacing $\alpha^b$ by $\alpha(z)$ and $[H^+]$ by $[H^+(z)] = [H^+]e^{-y(z)}$.

## III. Scaling-Type Approach

In a previous contribution,[9] the structure of a polyelectrolyte brush in which the segments have a fixed charge was analyzed in detail along the lines originally proposed by Borisov et al.[7,8] In that work, $m$ is the number of bonds between two charges along the chain. The charge density $1/m$ can thus be identified as a partial charge per segment. We will use the symbol $\alpha_0 \equiv 1/m$ to denote this constant degree of dissociation. We summarize some main conclusions for a constant-charge brush, concentrating on the effects of the salt concentration, expressed as the volume fraction $\phi_s$ of the cations. Unlike in refs 7 and 9, we use the symbol $\sigma$ for the grafting density (number of chains per area $d^2$), which is the inverse of the area per chain.

When the Debye screening length $\kappa^{-1}$ is much smaller than the brush thickness $H$, the mobile counterions of the charged groups are trapped within the brush. The ensuing osmotic pressure causes the brush to swell. At low $\phi_s$, this leads to the OsB regime, in which $H$ is independent of $\sigma$ and $\phi_s$ and proportional to the chain length $N$ and the square root of the charge density:[9]

$$H \sim N\alpha_0^{1/2} \quad \text{(OsB)} \tag{10}$$

As $\phi_s$ increases, salt penetrates into the brush and screens the electrostatic interaction. At a certain $\phi_s$ there is a transition from the OsB to the SB regime. Here the brush characteristics are similar to those of neutral brushes with, however, a larger excluded-volume parameter $v_{eff}$. In the neutral case the excluded-volume parameter $v = (1/2 - \chi)$ is of order unity. As shown in ref 9, the SB regime may be described by

$$H \sim N(\sigma v_{eff})^{1/3} \quad \text{(SB, QNB)} \tag{11}$$

where

$$v_{eff} = v + \alpha_0^2/\phi_s \tag{12}$$

The value of $\phi_s$ at the transition from OsB to SB is found by equating the expressions for $H$ given in eqs 10 and 11: $\alpha_0^{1/2} \sim (\sigma\alpha_0^2/\phi_s)^{1/3}$ or $\phi_s \sim \sigma\alpha_0^{1/2}$.

If $\phi_s$ is further increased, $v_{eff}$ decreases. Eventually the ratio $\alpha_0^2/\phi_s$ becomes of order unity, so that at $\phi_s \approx \alpha_0^2$ we reach the QNB regime, where $v_{eff} \approx v$ and eq 11 reduces to the well-known expression for a neutral brush; in this regime the electrostatic interactions are fully screened by the excess of salt.

Let us now consider what modifications of this picture become necessary if $\alpha$ is a function of the local pH. We

consider the brush as a homogeneous region with degree of dissociation $\alpha$, in equilibrium with a bulk solution where the (imaginary) degree of dissociation is $\alpha^b$. The assumption that the brush is uniform in polymer density and electrostatic potential is a serious one. However, this assumption has been used to describe uncharged brushes[2] as well as charged brushes with a constant charge density[7] and seems to predict qualitatively correct behavior for these systems.[5,9,21]

By comparison with the two-state approximation (eqs 5, 7, and 8), we may write $\alpha$ as:

$$\alpha = \frac{\alpha^b}{\alpha^b + (1-\alpha^b)e^{-y}} \tag{13}$$

where $y$ is now the ($z$-independent) electrostatic potential in the brush with respect to the bulk solution. It may be expressed in terms of the ratio $\phi_+/\phi_s$ between the counterions inside the brush and those in the bulk solution through the simple Boltzmann relation

$$e^{-y} \approx \phi_+/\phi_s \tag{14}$$

In the SB and QNB regimes, $y$ is close to zero and $\alpha \approx \alpha^b$. In these regimes eqs 11 and 12 apply, where $\alpha^b$ is substituted for $\alpha_0$. The only difference with the constant-charge brush is that $\alpha$ and $\alpha^b$ are determined by the external pH of the solution.

In contrast to this, there is a major difference between brushes with constant and variable change in the OsB regime. We may then approximate eq 14 by:

$$e^{-y} \sim \sigma\alpha^{1/2}/\phi_s \tag{15}$$

where we used the electroneutrality condition (for a block profile) $\phi_+ = \alpha\sigma N/H$ and substituted $H/N \sim \alpha^{1/2}$ according to eq 10. The counterion concentration inside the brush is now much higher than that in the bulk solution, which goes along with a large negative electrostatic potential. This potential drives the acid groups to associate with protons, and $\alpha$ decreases. This decrease is expressed quantitatively by eq 13. After substitution of eq 15 and replacing $\alpha^b/(1-\alpha^b)$ by $K_a/[H^+]$, we find an implicit equation for $\alpha$, which cannot easily be solved analytically:

$$\alpha^{-1} \sim 1 + \frac{[H^+]}{K_a}\frac{\sigma}{\phi_s}\alpha^{1/2} \tag{16}$$

An approximation for high $y$ (hence, low $\phi_s$ and low $\alpha$) is found by neglecting the term 1 in eq 16, resulting in

$$\alpha^{3/2} \approx \frac{K_a}{[H^+]}\sigma^{-1}\phi_s \quad (\text{low } \alpha) \tag{17}$$

Equation 17 shows clearly that the degree of dissociation, and hence the charge density of the brush, becomes very low when the salt concentration is small. In this paper we assume that the proton or hydroxide concentration can be neglected with respect to $\phi_s$. In reality the lowest level of the ionic strength is determined by the pH of the solution. The limiting behavior for $\phi_s \to 0$ does not result from any of the approximations we have made so far. It is the consequence of the following self-regulating mechanism: at $\phi_s \approx 0$, even a very small charge density in the brush generates a high potential and a correspondingly high local proton concentration, which opposes further dissociation. The result may seem somewhat counterintuitive; however, a similar phenomenon is known to take place in biochemistry. A protein solution that derives colloidal stability from (weak) charges on the proteins may flocculate at very low salt concentrations due to the fact that the molecules become uncharged and no longer repel one another.

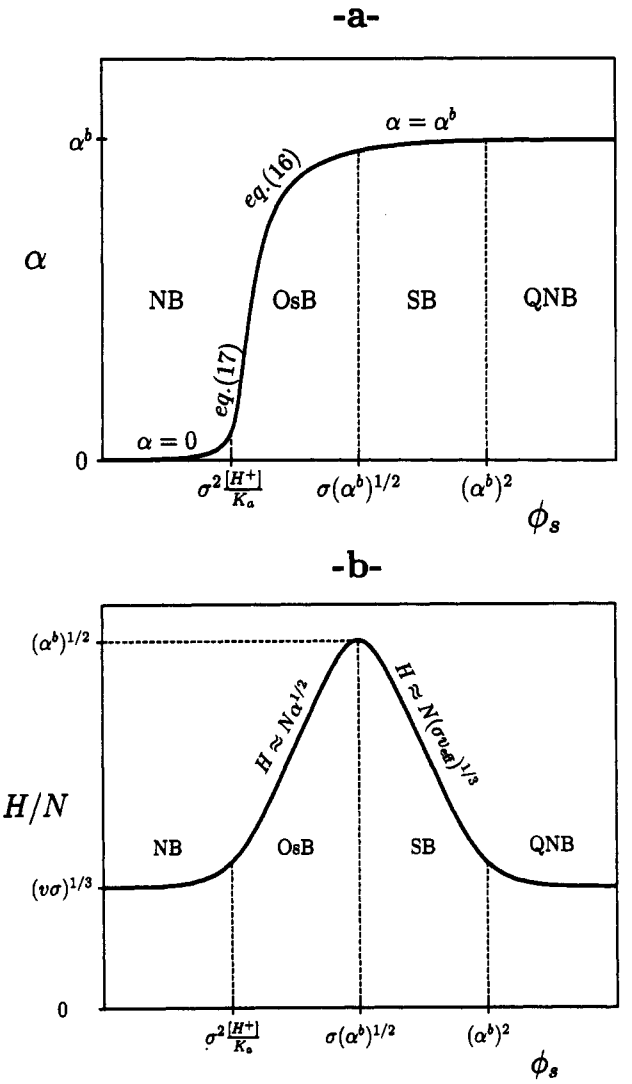


**Figure 1.** Schematic picture of the degree of dissociation $\alpha$ within the brush (a) and the brush thickness $H$ (b) as a function of the salt concentration $\phi_s$. In the NB regime $\alpha$ is close to zero; it increases in the OsB regime and reaches the constant (bulk) level $\alpha^b$ in the SB and QNB regimes. In the OsB regime, the dependence $\alpha(\phi_s)$ is given by eq 16; for low $\alpha$ the approximate eq 17 applies. The thickness, plotted as $H/N$, passes through a maximum as a function of the salt concentration. This maximum is located at the OsB/SB boundary.

The dependence of $\alpha$ on $\phi_s$ in the various regimes is summarized in Figure 1a. The QNB/SB and SB/OsB transitions are the same as those discussed for the constant-charge brush (with $\alpha_0$ replaced by $\alpha^b$). Upon further decreasing $\phi_s$ and thus reducing the screening of charges, a new transition takes place from the osmotic brush to a neutral brush (NB). (Note that this is only possible if the pH in solution allows one to go to such low $\phi_s$.) In this regime the electrostatic potential is so high that virtually all the groups are in the uncharged HA state, and the brush properties are essentially the same as for a fully neutral brush. As shown before for a brush with fixed charges,[9] the NB/OsB transition occurs at $\alpha \sim \sigma^{2/3}$ or, with eq 17, at $\phi_s \sim \sigma^2[H^+]/K_a$.

Figure 1b shows schematically how the brush thickness $H$ depends on $\phi_s$. In the NB and QNB regimes, the thickness is given by $H \sim N(\sigma v)^{1/3}$, where $v$ is of order unity in a good solvent. In the OsB regime $H \sim N\alpha^{1/2}$, where $\alpha$ increases with $\phi_s$ because the addition of salt

facilitates the dissociation of the acid groups. In the SB regime $H \sim N(\sigma v_{eff})^{1/3}$ according to eq 11, where $v_{eff} \sim 1/\phi_s$ so that the brush thickness decreases with increasing salt content, due to the screening of the charged groups. Hence, a maximum brush thickness is found at the transition between the OsB and SB regimes, at:

$$\phi_s^{max} \sim \sigma(\alpha^b)^{1/2} \tag{18}$$

At this maximum, the thickness equals the thickness of an osmotic brush with $\alpha = \alpha^b$:

$$H^{max} \sim N(\alpha^b)^{1/2} \tag{19}$$

## IV. Results

In this section we present numerical SCF results for the brush characteristics, and we compare them with the analytical predictions given in the previous section.

The numerical results were obtained for a hexagonal lattice with a lattice spacing $d = 0.6$ nm, using the two-state formalism discussed in the theory section. The relative dielectric permittivities were chosen as 80 for the solvent and 5 for all other substances. All calculations were performed for athermal systems. In the language of the Flory–Huggins model,[22] all $\chi$ parameters were taken to be zero. The value of $K_a$ was fixed at $10^{-7}$ M ($pK_a$ = 7) in order to be able to vary the salt concentration over a wide range; if the $pK_a$ had been chosen much lower, e.g., $pK_a$ = 4, no computations for salt concentrations below $10^{-4}$ M would have been possible. The salt concentration $\phi_s$ is expressed as a volume fraction; if desired, this value may be converted to a molarity by multiplying $\phi_s$ by $\sim$ 7.7 M. In the present implementation of the lattice model all monomers have an equal volume $v_{cell} = d^3$. Consequently, the molarity of pure water (clusters), pure salt, or pure polymer (on a monomer basis) equals $10^{-3}/(v_{cell}N_{av}) \approx 7.7$ M.

Figure 2a shows volume fraction profiles for a polyacid with chain length $N = 500$ and grafting density $\sigma = 0.002$, in equilibrium with a bulk solution at pH = 8 (equivalent to $[H^+]/K_a = 0.1$), at three widely different salt concentrations. For these parameters, the NB regime would be found below $\phi_s \approx 4 \times 10^{-7}$, the transition between OsB and SB is expected around $\phi_s \approx 2 \times 10^{-3}$, and the QNB regime would be reached only above $\phi_s \approx 0.8$. Hence, $\phi_s = 10^{-5}$ is in the lower end of the OsB regime, $10^{-3}$ is close to the OsB/SB transition, and $10^{-1}$ is in the upper end of the SB regime. In the latter case, the profile resembles the parabolic profile for a neutral brush. Despite the low anchoring density, the polymer is already fairly stretched: the profile extends over $\sim$90 layers, as compared to $(500)^{1/2} \approx 22$ for its radius of gyration. A fully screened brush would give a thickness of $500(0.001)^{1/3} \approx 50$ layers, so that at $\phi_s = 10^{-1}$ the screening is not yet complete.

At a lower salt concentration $\phi_s = 10^{-3}$ the increased electrostatic interaction causes a much stronger stretching and a much more dilute profile. However, a further decrease of $\phi_s$ to $10^{-5}$ causes the profile to shrink again because of a decreasing $\alpha$. This behavior, although unexpected at first sight, is in full agreement with the scaling predictions in section III. Since $\phi_s = 10^{-5}$ is still located in the OsB regime, the chains extend further into the solution than in the QNB or NB regimes, and the profile shape still deviates from a parabola. Nevertheless, Figure 2a shows clearly that with decreasing $\phi_s$ the brush characteristics approach those of a neutral brush.

In Figure 2b we plot the degree of dissociation of brush segments as a function of their distance to the surface, for the same set of parameters as in Figure 2a. The degree of dissociation tends to the bulk value $\alpha^b = 0.9$ at large

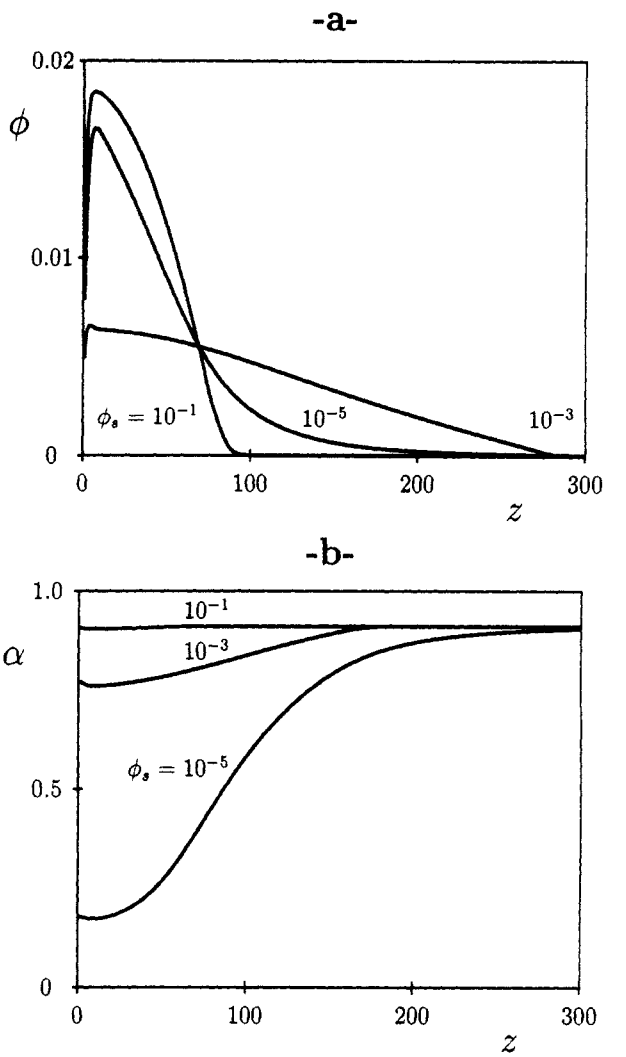


**Figure 2.** (a) Volume fraction profiles of a terminally anchored polyacid at three different salt concentrations (indicated) and the degree of dissociation $\alpha(z)$ of brush segments as a function of the distance to the surface (b). Parameters: $N = 500$, pH = 8, $pK_a = 7$, $\sigma = 0.002$.

distances from the surface, irrespective of $\phi_s$. In the salted brush (upper curve), virtually all brush segments have the maximum degree of dissociation $\alpha^b$, as expected. The neutral brush ($\phi_s = 10^{-5}$), on the other hand, consists mainly of segments that have a much lower degree of dissociation. The curve for $\phi_s = 10^{-3}$ corresponds to the most extended brush. In the scaling section we assumed that up to this point the segments in the brush remain maximally dissociated. The figure shows this to be true to a first approximation only. The observed deviation of $\alpha$ from $\alpha^b$ is expected to lead to a lower value for the maximum thickness than predicted by eq 19, as we will show below.

The next two figures illustrate the behavior of the average degree of dissociation in the brush and of the brush thickness as a function of the salt concentration $\phi_s$. These figures may be compared with the qualitative picture of Figure 1. Since the location of the boundary of a continuous brush profile is not unambiguous, we use the root-mean-square thickness $H_{rms}$ as a measure of $H$. It is defined as

$$H_{rms}^2 = \frac{1}{\theta}\sum_z z^2\phi(z) \tag{20}$$

where $\theta = N\sigma = \sum_z \phi(z)$ is the grafted amount per surface site. Although $H_{rms}$ is expected to be lower than $H$ as used in eqs 11 and 19, the trends in $H_{rms}$ and $H$ should be comparable.

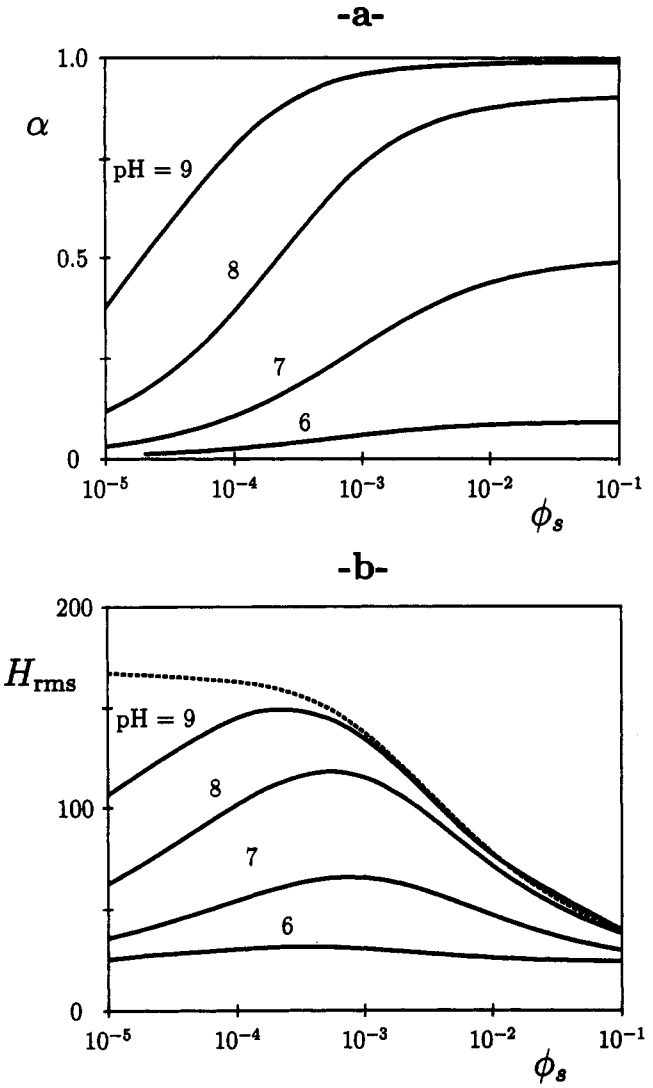


**Figure 3.** Degree of dissociation $\alpha$, averaged over all brush segments, as a function of salt concentration $\phi_s$ at four different pH values (a) and the dependence of the root-mean-square layer thickness $H_{rms}$ on $\phi_s$ (b). Parameters are the same as in Figure 2. The dotted curve in a represents the behavior of an equivalent conventional (pH-independent) charged brush.

In Figure 3a, we plot the average degree of dissociation $\alpha$ of brush segments as a function of the salt concentration, for four pH values. The theoretical prediction (Figure 1a) shows a more or less constant $\alpha = \alpha^b$ in the QNB regime at high $\phi_s$. With decreasing $\phi_s$ we enter the SB regime, where $\alpha$ is expected to remain constant down to the OsB/SB boundary. This boundary scales as $\sigma(\alpha^b)^{1/2}$, according to eq 18. If the numerical prefactors are assumed to be around unity, one would expect it to be situated at $\phi_s \approx 6 \times 10^{-4}$ for pH = 6. The SCF calculations show indeed that $\alpha$ begins to decrease around this value of $\phi_s$; the transition is, however, rather broad. The shift of this transition as a function of pH is related to the shift of the maximum brush thickness (plotted in Figure 3b) and we will return to this point below. For very low $\phi_s$, $\alpha$ decreases to low values, as expected. The NB regime (where $\alpha \approx 0$) is not reached for the higher pH values in Figure 3a. Nevertheless, the general trends of Figure 1 are well reproduced.

Figure 3b gives results for $H_{rms}$ as a function of $\phi_s$ for four pH values, at $N = 500$ and $\sigma = 0.002$ as before. All the curves show a maximum, as anticipated in Figure 1b. For comparison, the dotted curve in Figure 3b gives the equivalent results for a brush with a constant degree of dissociation ($\alpha^b = 1$).

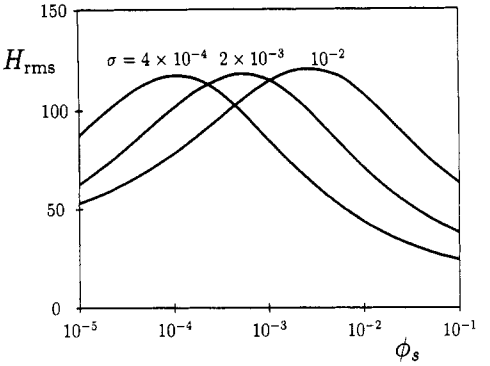


**Figure 4.** Root-mean-square layer thickness as a function of salt concentration at pH = 8 for three different anchoring densities (indicated). Other parameters are as in Figure 2.

The maxima in this figure are predicted to be located at the OsB/SB boundary. We may derive this location from the curve for the constant-charge brush (dotted curve), for which the OsB/SB boundary can be recognized as the salt concentration where the brush thickness (constant at low $\phi_s$) begins to decrease. In Figure 3b we find this boundary at $\phi_s \approx 5 \times 10^{-4}$, and the brush thickness equals $H_{rms} \approx 155$ at this point.

At pH = 9 the maximum thickness should be found around this same salt concentration. This is indeed the case. The height of the maximum is only slightly lower than the thickness of the constant-charge brush, as expected. Thus, the curve at pH = 9 follows the scaling prediction for a brush of a weak polyacid.

Lower pH values lead to lower $\alpha^b$ values according to eq 6, so we expect the location of the maximum to shift to lower $\phi_s$ values. The height is also expected to decrease. Surprisingly, we find that the maxima shift to higher $\phi_s$ values instead. The thickness drops much faster than the expected rate. These deviations are caused by a breakdown of the assumption $\alpha = \alpha^b$ in the SB regime. We elaborate on this point below.

The assumption $\alpha \approx \alpha^b$ is equivalent to omitting the factor $e^{-y}$ in $\alpha = 1/(1 + [H^+]e^{-y}/K_a)$; cf. eq 9. We note that both when $[H^+] \ll K_a$ and when $[H^+] \gg K_a$ this becomes a good approximation: in the first case we can safely omit $e^{-y}$ even when $-y$ is of order unity; the latter case leads to $\alpha^b \approx 0$ and $y$ is vanishing. When $K_a \approx [H^+]$, however, even a moderate electrostatic potential will cause $\alpha < \alpha^b$. Consequently we expect for pH $\approx pK_a$ that $\alpha$ already begins to decrease in the SB regime. For example, in the pH = 8 curve in Figure 3a we indeed find the salt concentration where $\alpha$ begins to decrease to be relatively high, clearly above the SB/OsB transition. The corresponding maximum in Figure 3b follows this shift into the SB regime, where its height $H^{max}$ is no longer given by the OsB expression (eq 10). It is much lower due to the partial screening of electrostatic interactions in the SB regime.

The boundaries NB/OsB at low $\phi_s$ and SB/QNB at high $\phi_s$ cannot be read easily from Figure 3b, because the transitions are rather gradual. Moreover, it is clear that the NB/OsB boundary must be found at $\phi_s$ values lower than the plotted range. Nevertheless, the tendency of the NB/OsB boundary to shift to lower $\phi_s$ and the SB/QNB boundary to higher $\phi_s$ with increasing $\alpha^b$ is fully corroborated.

In Figure 4 we consider the effect of the anchoring density and plot $H_{rms}$ vs $\phi_s$ curves for three values of the brush density $\sigma$. The agreement with Figure 1b as to the location of the maximum is perfect: increasing the anchoring density by a factor of 5 shifts the maximum to a 5 times higher salt concentration but leaves its height

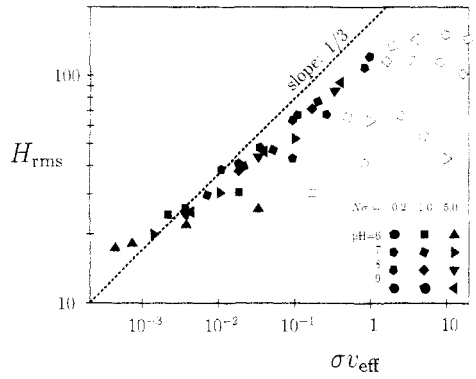


**Figure 5.** Root-mean-square layer thickness as a function of $\sigma v_{eff}$ for systems at three different grafting densities and four different pH's, as indicated in the caption. Systems corresponding to the SB and QNB regimes are indicated by filled symbols and those in the NB and OsB regimes by open symbols. In the latter two regimes ($\phi_s > \sigma(\alpha^b)^{1/2}$) a straight line with slope $^1/_3$ is expected according to eq 11.

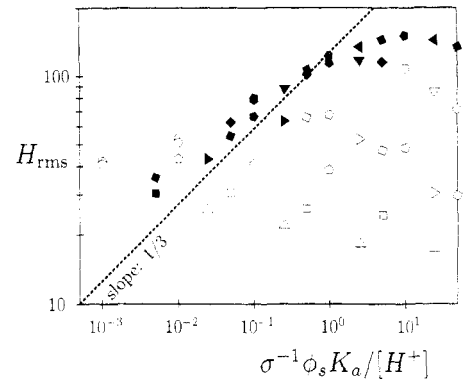


**Figure 6.** Root-mean-square layer thickness as a function of $\sigma^{-1}\phi_s K_a/[H^+]$ for the same systems as in Figure 5. The filled symbols correspond now to the OsB regime and the open ones to the other regimes. In the OsB regime ($\sigma^2[H^+]/K_a < \phi_s < \sigma(\alpha^b)^{1/2}$) eq 10 predicts a straight line with slope $^1/_3$.

unaffected. Note that in the OsB side of the curve (low $\phi_s$) $H \propto \sigma^{-1/3}$ whereas in the SB regime $H \propto \sigma^{1/3}$.

In Figures 3 and 4 we focused our comparison on the overall shape of the $H$ vs $\phi_s$ curve. Below we consider the variation of $H$ as a function of $\sigma$ and pH over a wide range of conditions. First, we check eq 11, describing the thickness in the combined SB and QNB regimes. Subsequently we compare the SCF calculations with analytical predictions for the OsB regime (eq 17). We do not make a comparison in the NB regime, since it would require calculations at extremely low salt concentrations. (At low ionic strength, the Debye screening length becomes very large so that we are forced to take a huge number of layers into account. In this case the convergence of the numerical equations is very poor.)

In Figure 5 we present calculations on the root-mean-square thickness of brushes at salt concentrations ranging from $\phi_s = 10^{-5}$ to $10^{-1}$, at three different anchoring densities and four different pH values. In the figure we plot the thickness as a function of $\sigma v_{eff}$ on a double-logarithmic scale, where $v_{eff}$ depends on the salt concentration $\phi_s$ according to eq 12. Different shapes and orientations of the symbols refer to different combinations of $\sigma$ and pH, as shown in the caption. Filled symbols represent systems in the SB or QNB regimes, whereas systems for which $\phi_s < \sigma(\alpha^b)^{1/2}$, corresponding to the NB and OsB regimes, are indicated by open symbols.

The filled symbols follow rather closely a straight line with slope $^1/_3$ (dashed line) as predicted by eq 11 for the SB and QNB regimes. The open symbols, on the other hand, are scattered throughout the picture (and some are outside the boundaries of the picture). They deviate strongly from the linear behavior.

For a brush in the osmotic regime, we expect the thickness to scale as $\alpha^{1/2}$ (eq 10). For low values of $\alpha$, its value may be approximated according to eq 17. Consequently, if we plot $H_{rms}$ as a function of the right-hand side of eq 17 on a log–log plot, we expect a straight line with slope $^1/_3$ for the data points corresponding to an osmotic brush with low $\alpha$.

This is verified in Figure 6, where we present the same data as in Figure 5, now as a function of $\sigma^{-1}\phi_s K_a/[H^+]$. In this case the OsB symbols are filled; the open symbols represent now the SB/QNB as well as the NB system. At first sight the agreement is less good in this case than in Figure 5. Some points indeed follow the predicted straight line. However, at high thickness the breakdown of the assumption $\alpha \ll 1$ causes downward deviations. At the other end of the OsB regime, the onset of nonelectrostatic excluded-volume interactions causes a thickness which is higher than predicted by eq 10.

These two figures can be summarized as follows. Using the expressions derived in the scaling section, data points in a wide range of parameters can be collected approximately onto two different master curves, one describing the behavior in the OsB regime (eq 10) and the other representing the combined SB/QNB behavior (eq 11). The most noticeable deviations from the master curve are a higher than expected thickness around the NB/OsB boundary due to nonelectrostatic excluded-volume interactions and a lower than expected thickness around the OsB/SB boundary, primarily due to a breakdown of the assumption $\alpha(z) = \alpha^b$ in the SB regime (used in Figure 5) and the approximating expression (17) for the OsB regime (used in Figure 6). Part of the disagreement is obviously due to the approximation of uniform polymer density and charge density in the brush. Although we believe this to be a secondary effect, it would be interesting to see the results of an improved analysis, starting from the parabolic potential profile.[23]

## V. Conclusions

We examined the thickness of a layer of grafted polyacids, i.e., a polyelectrolyte brush where the charge of each segment is a function of the local pH, and discussed it in terms of the known behavior of a constantly charged brush. The main conclusion of this study is that the thickness $H$ of such a brush passes through a maximum as a function of the salt concentration $\phi_s$, whereas the thickness of a "constant-charge" brush is a continuously decreasing function of salt concentration. This maximum is caused by the fact that at low $\phi_s$ (where a constant-charge brush reaches a plateau in its thickness) the weak groups associate with protons in order to minimize their electrostatic energy, so that the brush becomes virtually uncharged.

Assuming a block profile for the grafted layer and making first-order approximations for the degree of dissociation $\alpha$, we derived analytical expressions for the position (eq 18), as well as the height (eq 19), of this maximum. The dependence $H(\phi_s)$ on the right-hand side of the maximum was found to be the same as that for a constant-charge brush (eq 11). For the left-hand side a new (albeit approximate) expression was derived.

These analytical expressions for the location and height of the maximum, as well as the evolution of the thickness on either side of it, were checked using a SCF numerical model. The predictions on the location of the maximum, as well as on the thickness at high salt concentrations, were qualitatively fully corroborated. However, as the

SCF calculations showed, (over)simplifying assumptions on $\alpha$ around the maximum lead to an overestimation of the brush height. Furthermore, the thickness at low salt concentrations is only rather poorly described by the approximate scaling expression, due to the neglect of nonelectrostatic excluded-volume interactions.

## Appendix A. Two-State Model for Monomers

The statistical thermodynamics of chain molecules in inhomogeneous systems, wherein the polymer units can be in more than one state, was derived by Björling et al.[13,14] and simplified considerably by Hurter et al.[15] In both cases, this so-called two-state model was used to describe the behavior of poly(ethylene oxide) polymers in water. We apply it to the acid–base equilibrium of polyacids. In this appendix we present yet another derivation of the two-state model.

We consider the following system: a monomer of type A, that can be in either one of two states A1 and A2. For this case, eqs 5 and 7 can easily be obtained, as we show below. The key point in our derivation is that we view this system in two ways.

We may treat the monomer A as one type of monomer, which can be in several states. For monomers, the segment weighting factor $G_A(z)$ equals the ratio of the concentrations in layer $z$ and in the bulk:

$$G_A(z) = \phi_A(z)/\phi_A^b = \sum_{j=1,2} \phi_{Aj}(z)/\sum_{j=1,2} \phi_{Aj}^b \quad \text{(A1)}$$

Alternatively, we may consider the states A1 and A2 to be individual molecules. Then we define individual weighting factors as:

$$G_{Aj}(z) = \phi_{Aj}(z)/\phi_{Aj}^b \quad \text{(A2)}$$

with $j = 1, 2$. Inserting eq A2 in eq A1 and introducing the degree of dissociation $\alpha_i^b$ in the bulk solution:

$$\alpha_{Ai}^b = \phi_{Ai}^b/\sum_{j=1,2} \phi_{Aj}^b \quad \text{(A3)}$$

we immediately arrive at:

$$G_A(z) = \sum_{j=1,2} \alpha_{Aj}^b G_{Aj}(z) \quad \text{(A4)}$$

and the degree of dissociation in layer $z$ (defined analogously to $\alpha^b$) is found as:

$$\alpha_{Aj}(z) = \alpha_{Aj}^b G_{Aj}(z)/G_A(z) \quad \text{(A5)}$$

It is easy to see that eq A4 is a general form of eq 5 as used in the text. Similarly, eq A5 is a generalization of eq 7. Both equations are identical to the ones derived by Hurter for polymeric systems.

## References and Notes


(1) Halperin, A.; Tirrell, M.; Lodge, T. P. *Adv. Polym. Sci.* **1991**, *100*, 31.
(2) Alexander, S. *J. Phys. (Paris)* **1977**, *38*, 983. De Gennes, P.-G. *J. Phys. (Paris)* **1976**, *37*, 1445. De Gennes, P.-G. *Macromolecules* **1980**, *13*, 1069.
(3) Milner, S. T.; Witten, T. A.; Cates, M. E. *Macromolecules* **1988**, *21*, 2610.
(4) Zhulina, E. B.; Borisov, O. V.; Priamitsin, V. A. *J. Colloid Interface Sci.* **1990**, *137*, 495.
(5) Zhulina, E. B.; Borisov, O. V.; Priamitsin, V. A.; Birshtein, T. M. *Macromolecules* **1991**, *24*, 140.
(6) Pincus, P. *Macromolecules* **1991**, *24*, 2912.
(7) Borisov, O. V.; Birshtein, T. M.; Zhulina, E. B. *J. Phys. II* **1991**, *1*, 521.
(8) Zhulina, E. B.; Borisov, O. V.; Birshtein, T. M. *Polym. Prepr. (Am. Chem. Soc., Div. Polym. Chem.)* **1993**, *34*.
(9) Israëls, R.; Fleer, G. J.; Leermakers, F. A. M.; Zhulina, E. B., accepted for publication in *Macromolecules*.
(10) Evers, O. A.; Scheutjens, J. M. H. M.; Fleer, G. J. *J. Chem. Soc., Faraday Trans.* **1990**, *86*, 1333.
(11) Israëls, R.; Scheutjens, J. M. H. M.; Fleer, G. J. *Macromolecules* **1993**, *26*, 5405.
(12) Böhmer, M. R.; Evers, O. A.; Scheutjens, J. M. H. M. *Macromolecules* **1990**, *23*, 2288.
(13) Björling, M.; Linse, P.; Karlström, G. *J. Phys. Chem.* **1990**, *94*, 471.
(14) Linse, P.; Björling, M. *Macromolecules* **1991**, *24*, 6700.
(15) Hurter, P. N.; Scheutjens, J. M. H. M.; Hatton, T. A. *Macromolecules* **1993**, *26*, 5030.
(16) Fleer, G. J.; Cohen Stuart, M. A.; Scheutjens, J. M. H. M.; Cosgrove, T.; Vincent, B. *Polymers at Interfaces*; Chapman and Hall: London, 1993.
(17) Scheutjens, J. M. H. M.; Fleer, G. J. *J. Phys. Chem.* **1979**, *83*, 1619.
(18) Scheutjens, J. M. H. M.; Fleer, G. J. *J. Phys. Chem.* **1980**, *84*, 178.
(19) Cosgrove, T.; Heath, T.; van Lent, B.; Leermakers, F. A. M.; Scheutjens, J. M. H. M. *Macromolecules* **1987**, *20*, 1692.
(20) Barneveld, P. A.; Hesselink, D. E.; Leermakers, F. A. M.; Scheutjens, J. M. H. M.; Lyklema, J. *Langmuir*, in press.
(21) Wijmans, C. M.; Scheutjens, J. M. H. M.; Zhulina, E. B. *Macromolecules* **1992**, *25*, 2657.
(22) Flory, P. J. *Principles of Polymer Chemistry*; Cornell University Press: Ithaca, NY, 1953.
(23) Zhulina, E. B. Work in progress.